

## ***Electronic Supplementary Information (ESI)***

### **Distinguishing the Influence of Structural and Energetic Disorder on Electron Transport in Fullerene Multi-Adducts**

*Florian Steiner, Samuel Foster, Arthur Losquin, John Labram, Thomas D. Anthopoulos,  
Jarvist M. Frost<sup>†\*</sup>, Jenny Nelson<sup>1</sup>*

Department of Physics and Centre for Plastic Electronics, Imperial College London, London  
SW7 2AZ, UK

<sup>†</sup> Now at Department of Chemistry, University of Bath, Bath BA2 7AY, UK

---

<sup>1</sup> Corresponding authors: [jenny.nelson@imperial.ac.uk](mailto:jenny.nelson@imperial.ac.uk); [j.m.frost@bath.ac.uk](mailto:j.m.frost@bath.ac.uk)

## **Content**

SI1. Temperature-dependent field-effect-transistor measurements of electron-mobilities

SI2. Time of flight measurements

SI3. MD-structures of PCBM, bis-PCBM and tris-PCBM

SI4. Coarse-grained vs. atomistic RDF

SI5. Fullerene side-chain enumeration

SI6. Small MD structures

SI7. Reorganisation energy

SI8. Charge transfer integrals

SI9. Discrete energy levels for isomers

SI10. Disorder conversion

SI11. Full table of charge-carrier mobilities for large MD structures

SI12. Coarse grain fullerene force field

SI13. References for supporting information

## SI1. Temperature-dependent field-effect-transistor measurements of electron-mobilities

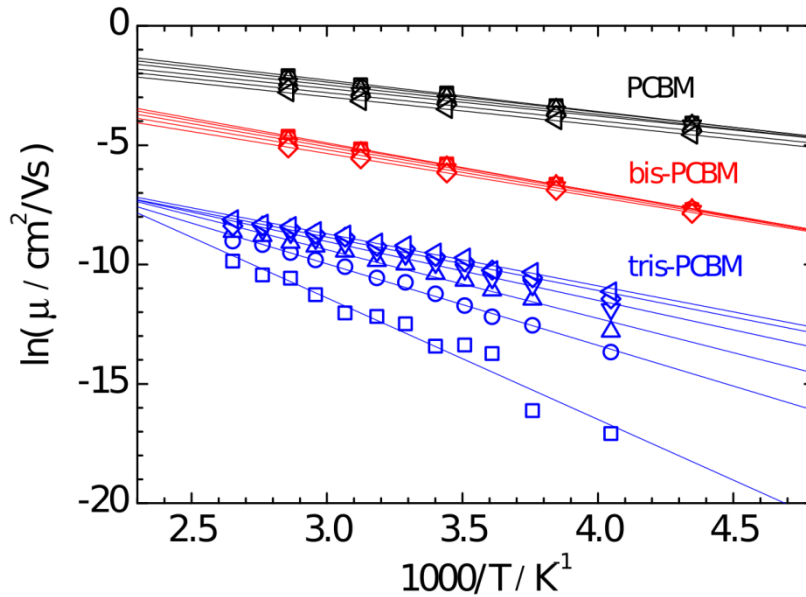


**Figure SI1.** Temperature-dependent electron field-effect mobilities measured with bottom-gate top-contact field-effect transistors. The gate voltages shown for PCBM are 20 V (squares), 25 V (circles), 30 V (up triangles), 35 V (down triangles), 40 V (diamonds) and 45 V (left triangles); for bis-PCBM 25 V (squares), 30 V (circles), 35 V (up triangles), 40 V (down triangles) and 45 V (diamonds); for tris-PCBM 30 V (squares), 40 V (circles), 50 V (up triangles), 60 V (down triangles), 70 V (diamonds) and 80 V (left triangles).

## **Conversion of disorder parameter from Gaussian Disorder Model to density of states broadening**

A way to investigate the relative importance of structural in energetic disorder are temperature dependent measurements. In high temperature limit the effect of energetic disorder diminishes as charge transfer over potential barriers and traps is thermally activated whereas the influence of configurational disorder persists. Further, an effective energetic disorder can be extracted from the Gaussian Disorder Model (GDM)<sup>8</sup>.

Previously, field-effect transistor (FET) measurements have been successfully applied to quantify mobilities of PCBM and bis-PCBM at room temperature<sup>5,6</sup>. For FET structures, the measurements are carried out on thin films which allows the study of pristine films without PS (in contrast to the time-of-flight measurements). More importantly, the quantification of the mobility does not rely on a transient feature but a steady current flow which is easier to achieve.

We employed bottom-gate top-contact FETs at a range of gate-voltages  $V_G$  (see Fig. 1). At room temperature and  $V_G = 30$  V, PCBM shows a mobility of  $5 \times 10^{-2}$  cm<sup>2</sup>/Vs, bis-PCBM a mobility of  $3 \times 10^{-3}$  cm<sup>2</sup>/Vs and tris-PCBM a mobility of  $3 \times 10^{-5}$  cm<sup>2</sup>/Vs. Mobilities determined from organic FETs show at sufficiently high temperatures an Arrhenius type temperature dependence  $\ln \mu \propto -E_a/k_B T$  which is incompatible with the GDM used for the time-of-flight data.

An alternative route to gain insight concerning the energetic disorder in FETs is the characteristic activation energy  $E_a$  which measures the average energy that an electron needs to hop between neighbouring transport sites.  $E_a$  is gate-voltage dependent as with higher  $V_G$  more states are thermally accessible which reduces  $E_a$ .<sup>3</sup>  $E_{a, \text{tris}}$  ranges from 190 to 360 meV as  $V_G$  decreases from 80 V to 30 V,  $E_{a, \text{bis}}$  ranges from 155 to 180 meV as  $V_G$  decreases from 50 V to 25 V and  $E_{a, \text{mono}}$  ranges from 100 to 110 meV as  $V_G$  decreases from 45 V to 20 V. As expected  $E_a$  decreases when  $V_G$  increases. Clearly,  $E_a$  is increasing in the order  $E_{a, \text{tris}} < E_{a, \text{bis}} < E_{a, \text{mono}}$ .

As previously discussed, the effect of energetic disorder diminishes in the limit of high temperatures. When extrapolating the FET mobility data at fixed gate voltage  $V_G = 40$  V all three fullerene derivatives show infinite-temperature mobilities of 1.5 - 1.9  $\text{cm}^2/\text{Vs}$  which is within the experimental errors. This indicates that structural disorder is of minor importance compared to the energetic disorder introduced by isomeric variations in LUMO levels which is in agreement with the findings in the simulations.

## SI2. Time of flight measurements

Optically thick films ( $> 1 \mu\text{m}$ ) of PCBM and the higher adducts are typically rough and mechanically unstable. Therefore, we followed the method of previous work<sup>7</sup> dispersing the fullerene in an 'inert' matrix of polystyrene (PS) by codeposition. Given that PCBM tended to agglomerate in PCBM:PS blends when exceeding 40 wt%, temperature dependent ToF measurements at an applied bias of  $7 \times 10^5 \text{ V/cm}$  were carried out on films with 33 wt% PCBM. As the measured transients are highly dispersive we extracted electron mobilities with the integral method<sup>8</sup>. From the Gaussian Disorder Model (GDM)<sup>4</sup> we derive an energetic disorder of  $\sigma = 77 \text{ meV}$  which is in good accordance with literature<sup>9</sup>. For bis- and tris-PCBM the ToF transients were too dispersive to reliably obtain mobilities.

### S3. MD-structures of PCBM, bis-PCBM and tris-PCBM

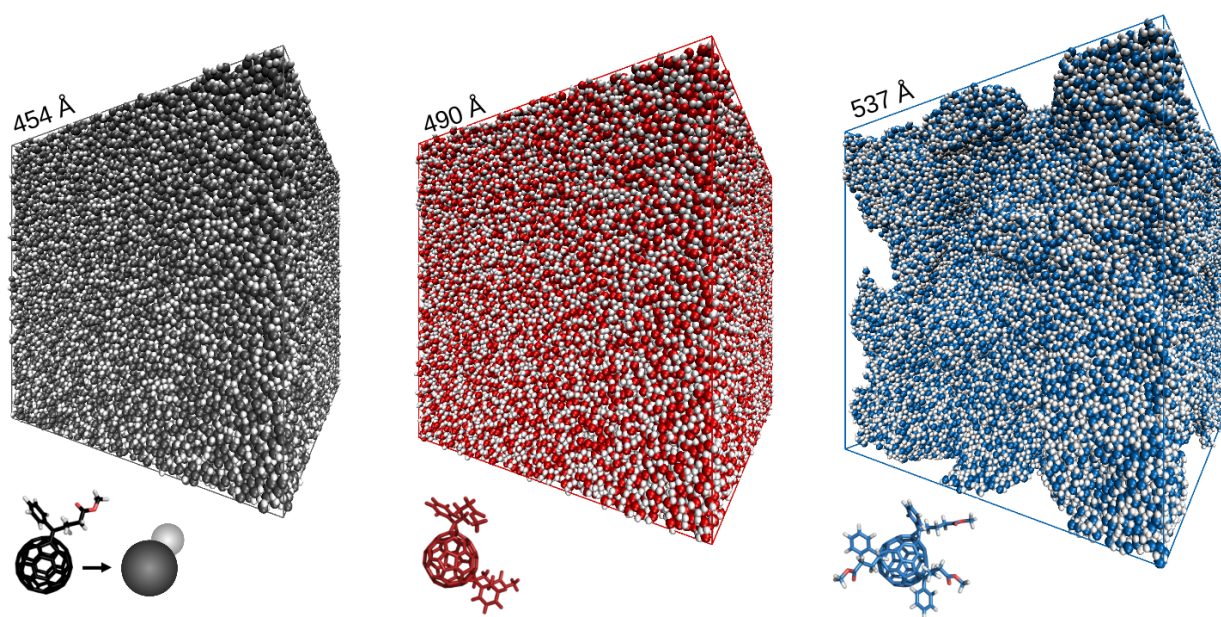


**Figure S13.** Representative coarse-grained MD structures containing 100,000 molecules. a) PCBM, b) bis-PCBM and c) tris-PCBM.

## SI4. Coarse-grained vs. atomistic RDF

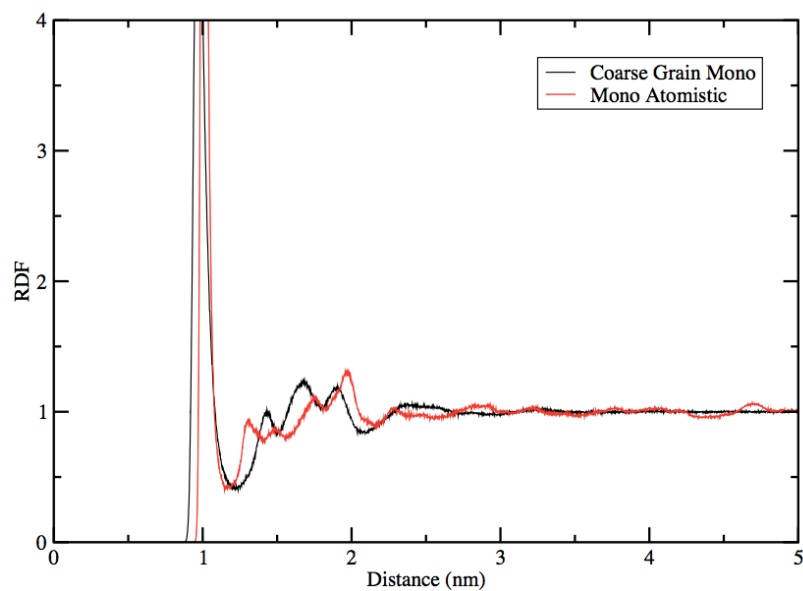


**Figure SI4A.** Radial distribution functions (RDF) of PCBM assemblies generated by atomistic molecular dynamics (Atomistic) and coarse-grain molecular dynamics (Coarse Grain). Those two RDFs were used to fit the force field parameters of the coarse-grain model.

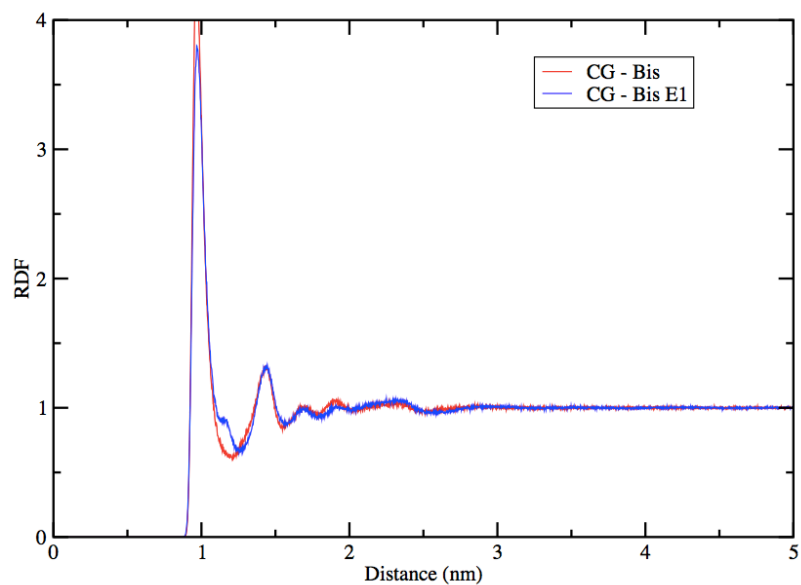


**Figure SI4B.** Radial distribution functions (RDF) of coarse-grained (CG) assemblies of isomeric mixes of bis-PCBM and of one bis-PCBM isomer E1.

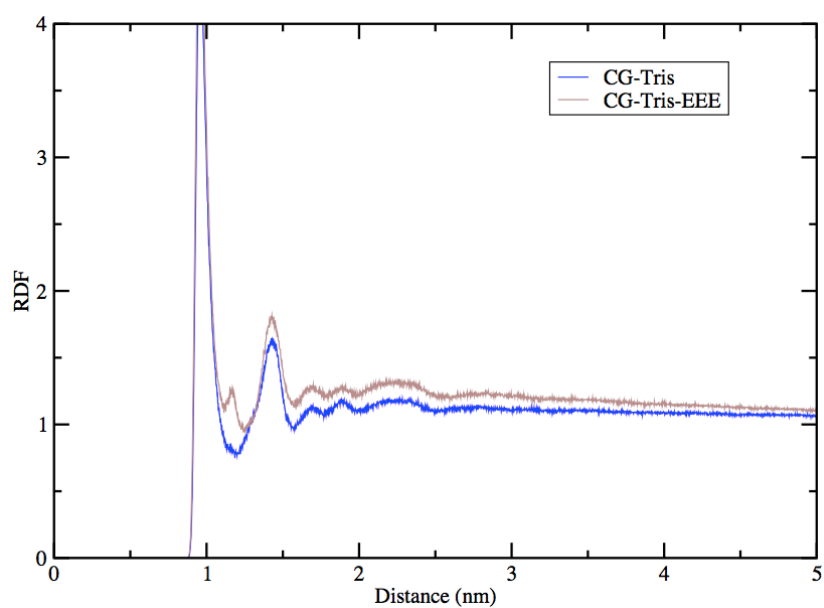


**Figure SI4C.** Radial distribution functions (RDF) of coarse-grained (CG) assemblies of isomeric mixes of tris-PCBM and of one tris-PCBM isomer EEE.

## SI5. Fullerene side-chain enumeration

C60 has 90 bonds between the 60 atoms. 30 of these are 6,6 coordinating (1.37 Å long - along two hexagonal facets) and have more double-bond like character. The remaining 60 bonds are 5,6 coordinating (1.448 Å long). PCBM is formed by 4+2 cycloaddition. These sidechains are believed to wholly coordinate with the 6,6 bonds.

The 8 unique bis isomers, and 45 tris isomers, have been identified and their point group derived in previous work. However we did not find a computationally readable list of structures which would be directly useful in constructing our coarse grained model.

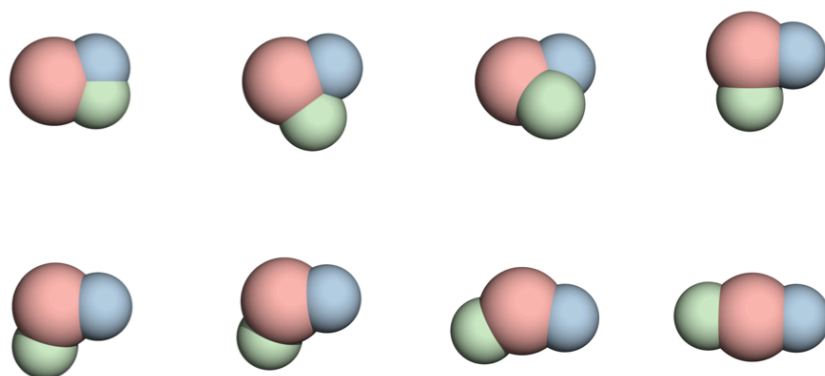


**Figure SI5A.** The 8 unique bis isomers, at the coarse grain level. From left to right the isomers are: C1, C2, C3, E, T4, T3, T2, T1.

The bis isomers can be enumerated (identified) by hand and are defined in our coarse grain model simply as the internal angle between the two side chains. Of the 9 unique isomers, two are equatorial, which for our coarse grain model results in equivalent 90-degree angles.

Identifying unique tris isomers is much more difficult, so we developed a computational method to directly enumerate the isomers and calculate the coarse-grain specification of angles between the three sidechains.

First we read in the coordinates of a C60 molecule with (0,0,0) defined as the centre of the fullerene. We then identify the 6,6 bonds by spacing ( $<1.4\text{\AA}$ ) between atoms. The midpoint of these bonds, and thus the attachment point of the sidechains, was found by averaging the Cartesian positions of the two bonded atoms.

We can then enumerate over all possible permutations of these bonds (30 options, 3 selections leading to 24360 permutations, which can be immediately simplified by inspection to 812 permutations by taking 2 selections of 29 options if we choose the first location for the first sidechain). Three inter-sidechain angles are then generated (arccos of the dot product) from these sets of 3 coordinates (a,b;a,c;b,c).

As the order in which we specify the inter-sidechain angles does not matter, we are free to rearrange. By reordering these angles in ascending order, we can identify degenerate configurations by direct comparison.

The newly calculated set of three angles is compared against a list of uniquely defined isomers, and either appended to this list if found to be unique, or discarded and the degeneracy counter of that (already identified) isomer incremented.

Isomer	$\theta_{A,B}$	degeneracy
E	90	4
C2	60	4
C3	72	4
C1	36	4
T3	144	4
T4	108	4
T2	120	4
T1	180	1

**Table SI5A.** Inter-sidechain angles for bis isomers, degeneracy from number of ways possible of constructing this unique isomer. All isomers have the same 4-fold degeneracy due to the C4 symmetry of bond location, except for the T1 isomers

With a simple bit of trigonometry and enumeration we directly discover the 45 unique tris isomers and their symmetry derived degeneracy, and can directly generate the angle specification suitable for an empirical force field specification, and a relaxed set of coarse grain coordinates for visualisation and the generation of a dense initial structure for molecular dynamics.

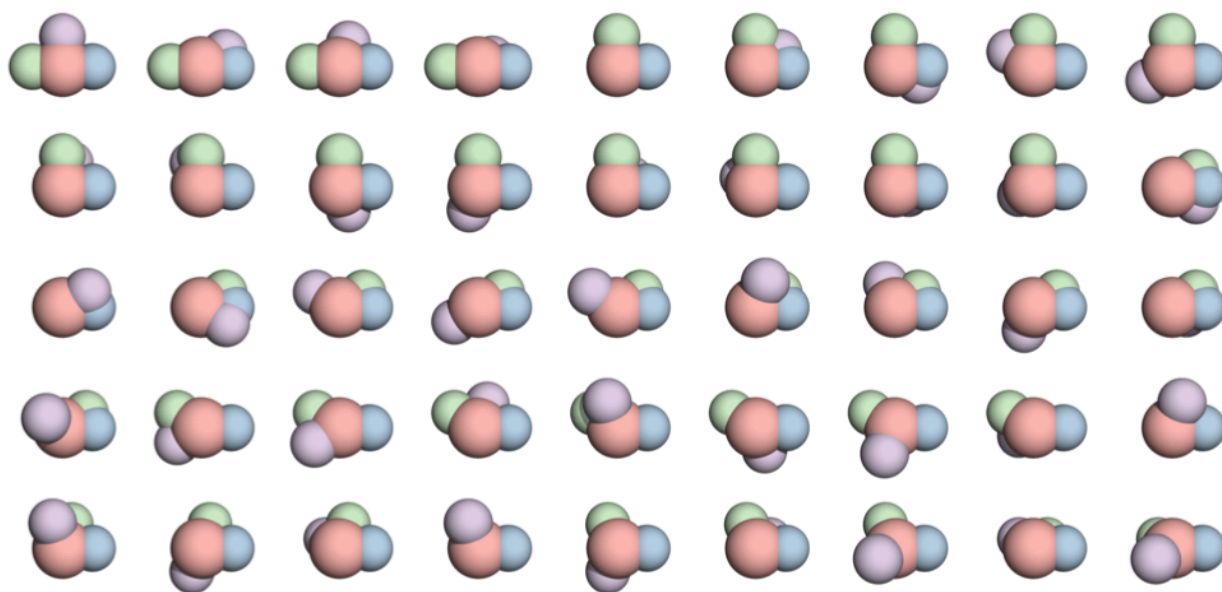


**Figure SI5B.** The 45 unique tris isomers, at the coarse grain level, as generated automatically by the method described here.

$\theta_{A,B}$	$\theta_{A,C}$	$\theta_{B,C}$	degeneracy
36	36	36	1
36	36	60	3
36	36	72	3
36	60	60	3
36	60	72	6
36	60	90	6
36	72	90	6
36	72	108	6
36	90	108	6
36	90	120	6
36	108	120	6
36	108	144	6
36	120	120	3
36	120	144	6
36	144	144	3
36	144	180	6
60	60	108	3
60	60	120	3
60	72	72	3
60	72	90	6
60	72	120	6
60	90	108	6
60	90	144	6
60	108	108	3
60	108	144	6
60	120	144	6
60	120	180	6
60	144	144	3
72	72	108	3
72	72	144	3
72	90	120	6
72	90	144	6
72	108	120	6
72	108	180	6
72	120	144	6
72	144	144	3
90	90	90	2
90	90	180	3
90	108	120	6
90	108	144	6
90	120	144	6
108	108	108	1
108	108	144	3
108	120	120	3
120	120	120	1

**Table S15B.** Inter-sidechain angles for all 45

enumerated tris isomers, with a statement of the degeneracy (number of ways possible of constructing this unique isomer).

## SI6. Small MD structures

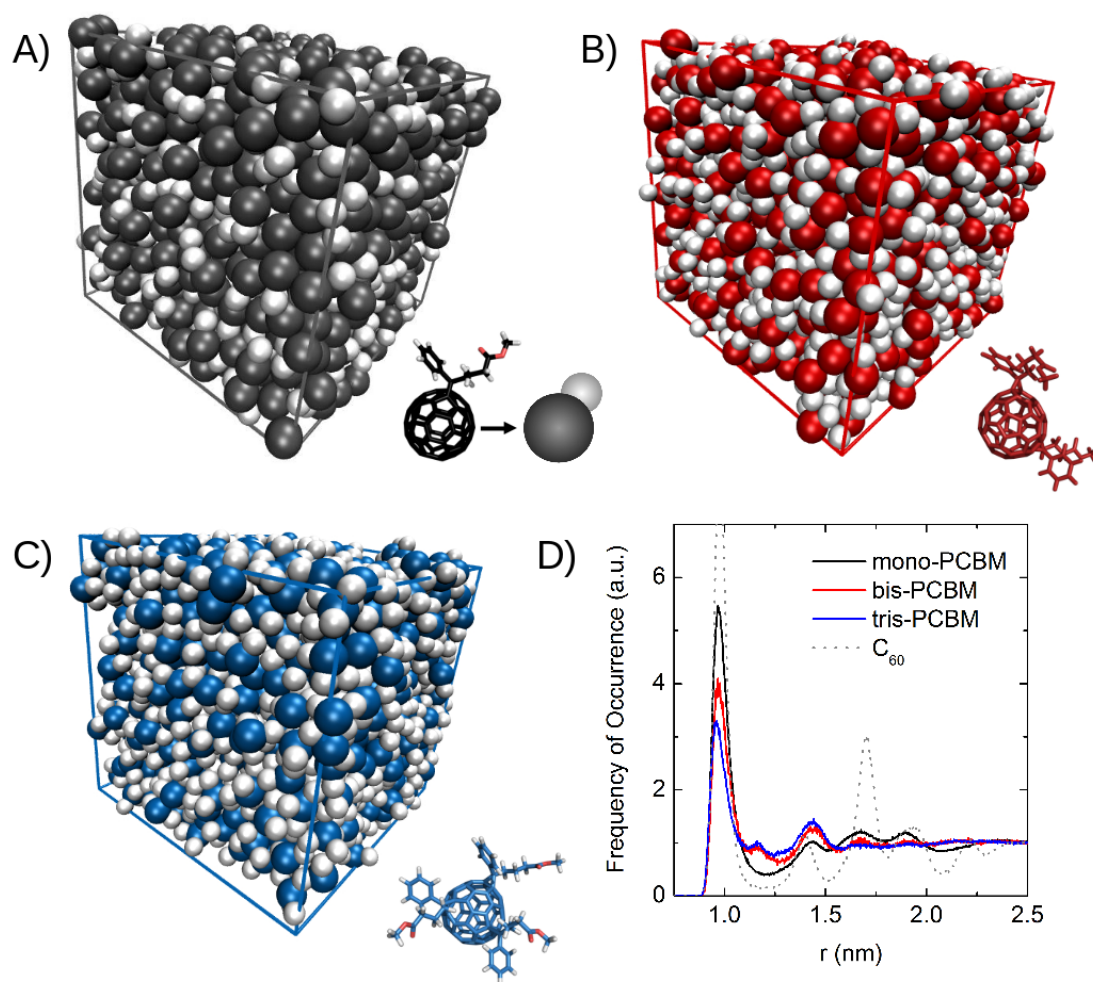


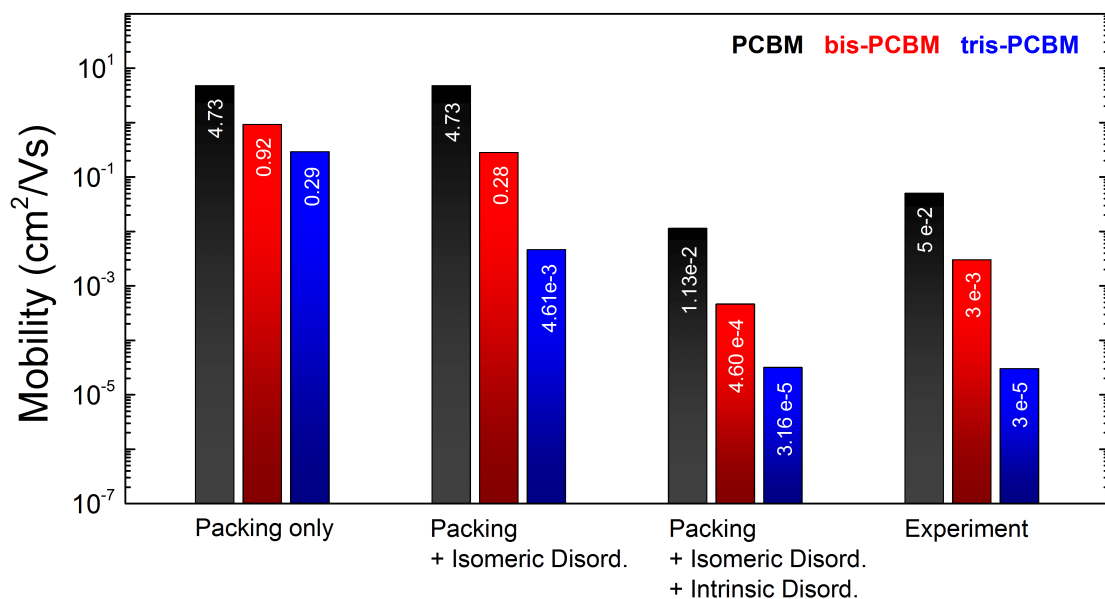
**Figure SI6A.** Small MD structures built of 1,000 molecules. A) PCBM, B) bis-PCBM and C) tris-PCBM. D) Radial distribution function of C<sub>60</sub> and the structures in A)-C).

100,000 molecules		M	B	T	B-E1	T-EEE
Packing disorder only	$\sigma$ (meV)	0	0	0	0	0
	$\mu$ (cm <sup>2</sup> /Vs)	4.75	1.22	4.87e-1	6.55e-1	2.61e-1
Isomeric disorder	$\sigma$ (meV)	0	56	121		
	$\mu$ (cm <sup>2</sup> /Vs)	4.75	2.78e-1	1.31e-3		
Isomeric & implicit disorder	$\sigma$ (meV)	135	146	181		
	$\mu$ (cm <sup>2</sup> /Vs)	9.23e-3	5.67e-4	8.80e-6		

1,000 molecules		M	B	T
Packing disorder only	$\sigma$ (meV)	0	0	0
	$\mu$ (cm <sup>2</sup> /Vs)	4.73	9.18e-1	2.88e-1
Isomeric disorder	$\sigma$ (meV)	0	56	121
	$\mu$ (cm <sup>2</sup> /Vs)	4.73	2.82e-1	4.61e-3
Isomeric & implicit disorder	$\sigma$ (meV)	187	196	223
	$\mu$ (cm <sup>2</sup> /Vs)	1.13e-2	4.60e-4	3.16e-5

**Table SI6.** Results for simulated mobility  $\mu$  for all cases studied for both large (100,000 molecules) and small (1,000 molecules) molecular assemblies. The value of  $\sigma$  represents the energetic disorder applied for each fullerene type and each level of disorder simulated (i.e., packing disorder only, isomeric disorder, isomeric and implicit disorder). For all calculations a reorganization energy of  $\lambda = 200$  meV is assumed.



**Figure SI6B.** Simulated charge transport data for reorganisation energies of  $\lambda = 200$  meV and structures containing 1,000 molecules. The bar chart compares the experimental results with the three different levels of disorder studied. Although the average mobility values of small and large MD structures compare very well, the variation increases. While the standard deviation for large structures stayed below 1% in all cases, mobilities from small structures can vary by more than an order of magnitude due to the large energetic disorder.

## SI7. Reorganisation energy

In order to evaluate the influence of the reorganisation energy on charge transport, internal reorganisation energies of all distinct fullerene multi-adduct isomers have been calculated with the four-point method described in reference<sup>1</sup>. The average internal reorganisation energies  $\lambda_{in}$  are 155 meV for PCBM, 229 meV for bis-PCBM and 254 meV for tris-PCBM.

	LUMO (eV)	$\lambda_{in}$ (meV)
PCBM	-3.749	155
bis-C1	-3.678	294
bis-C2	-3.646	267
bis-C3	-3.645	165
bis-E	-3.619	178
bis-T1	-	290
bis-T2	-3.712	161
bis-T3	-3.578	292
bis-T4	-3.543	183
tris-EEE	-3.240	214
tris-EET11	-3.444	200
tris-EET12	-3.590	193
tris-ET3T2	-3.436	187
tris-ET4T2	-3.474	205
tris-ET4T3	-3.528	201
tris-T3T3T3	-3.260	312
tris-T4T3T3	-3.390	427
tris-T4T4T2	-3.590	297
tris-T4T4T4	-3.509	303

**Table SI7.** LUMO energies and internal reorganization energies  $\lambda_{in}$  of fullerene PCBM and its multi-adducts.

Marcus hopping rates  $\Gamma$  (see equation 1 in main text) are calculated for all possible pairwise combinations of isomers.  $\Gamma$  is calculated for both (a) individual internal reorganisation energies  $\lambda_{\text{in, indiv.}}$  as shown in Table SI7 and (b) for identical reorganisation energies  $\lambda_{\text{in, paper}} = 200$  meV as assumed in the main paper. Comparing the two cases by dividing the hopping rates  $\Gamma_{\text{indiv}} / \Gamma_{\text{paper}}$ , we find values between 0.3 and 4 (maximum of 4 for tris-T3T3T3 and tris-T4T3T3) which is small compared to the variations in experimental mobilities between fullerene adducts.

Thus, we can conclude that the isomer-dependent internal reorganisation energies  $\lambda_{\text{in}}$  are insufficient to explain the experimental mobilities which differ by orders of magnitude. Since the average internal reorganisation energy increases when going to the next higher adduct,  $\lambda_{\text{in}}$  might contribute to the mobility spreading between mono-, bis- and tris-PCBM.

## SI8. Charge transfer integrals

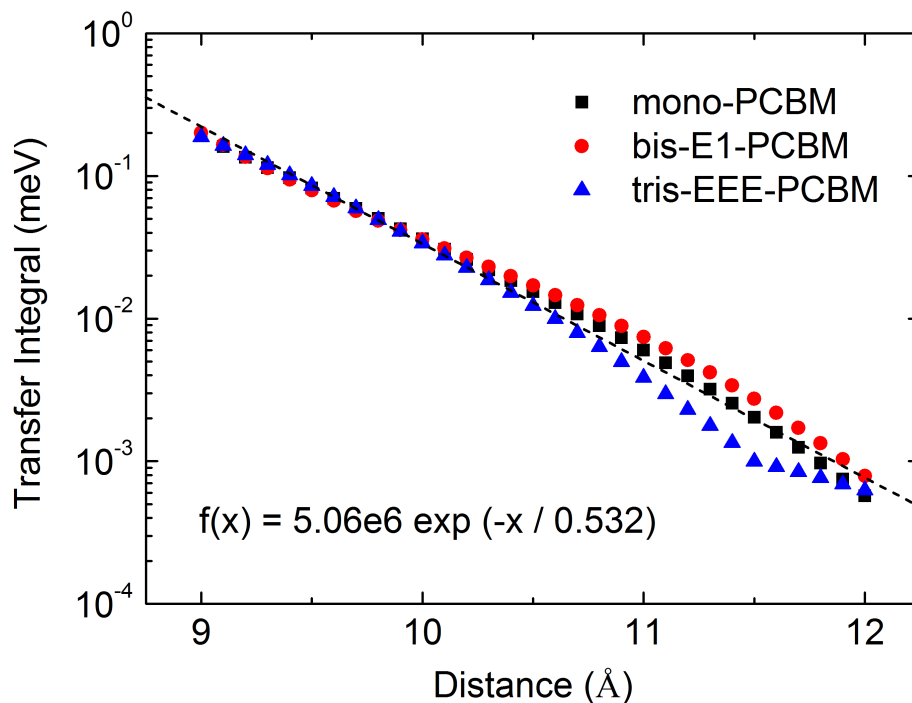


**Figure SI8.** Charge transfer integrals of PCBM, bis-E1-PCBM and tris-EEE-PCBM calculated with the projective method<sup>2</sup>. The electronic structure of the molecules was calculated with the hybrid functional b3lyp and the 6-31g\* basis set. For our simulation we approximate the characteristic length  $d$  to be  $0.5 \text{ \AA}$  (instead of  $0.532 \text{ \AA}$ ) agreeing with our previous study on  $C_{60}$ <sup>3</sup>. We then adjust the prefactor to  $15 \text{ keV}$  so that  $J(10 \text{ \AA})$  agrees with the simulated data ( $J(10 \text{ \AA}) = 30 \text{ meV}$ ).

## SI9. Discrete energy levels for isomers

So far, we have discussed the influence of isomeric disorder using a Gaussian density of states. In this chapter, discrete energy levels are assigned to each isomer type. In the MD generated assemblies there is an equal number of all isomer types. For bis-PCBM all LUMO levels as calculated by Frost et al. (2010) are assigned to the relevant isomer in our MD molecular assemblies. For tris-PCBM only ten out of 45 (total number of different isomer types) LUMO energies are known – we therefore assign an equal distribution of those ten energies to the MD structures.

Because the distribution is unknown, choosing Gaussian rather than discrete energies makes results less sensitive to the exact fraction of low LUMO isomers.

Different levels of disorder are considered in the simulation; 1) packing only, 2) packing and isomeric disorder, 3) packing, isomeric disorder and intrinsic disorder. The results of the charge transport calculations are shown in Figures SI9. Compared to the case of Gaussian DOS, simulations with discrete isomer energies exhibit five times lower electron mobilities.

The reason for this is most likely the comparably high fraction of low LUMO isomers which act as traps for equally distributed, discrete site energies.

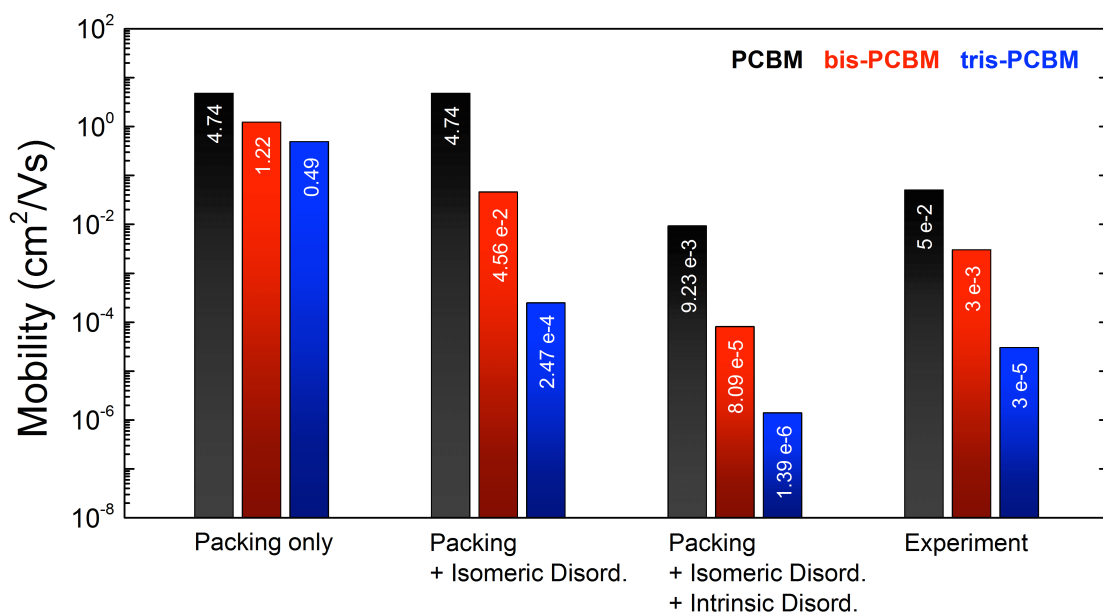


Figure S19. Simulated charge transport data for reorganisation energies of  $\lambda = 200$  meV and structures containing 100,000 molecules. Energies of isomers are assigned discretely. Bar chart compares the experimental results with the three different levels of disorder studied.

## SI10. Disorder Conversion

The commonly accepted method to extract the energetic disorder  $\sigma_{\text{GDM}}$  from experimental, temperature-dependent mobilities is the Gaussian Disorder Model (GDM)<sup>4</sup>. Essentially, the GDM is a set of empirical formulas based on Miller-Abrahams hopping rates. In our simulation, we use Marcus hopping rates where the energetic disorder  $\sigma$  is introduced in the site energy  $E$  (see equation 1). As both hopping mechanisms are based on differing physics,  $\sigma_{\text{GDM}}$  can not be directly transferred into  $\sigma$ .

A way to relate both types of disorder ( $\sigma_{\text{GDM}}$  and  $\sigma$ ) is to simulate temperature-dependent time-of-flight transients with varied energetic disorders  $\sigma$ . For each combination of temperature  $T$  and Gaussian density of states with width  $\sigma$  we simulate 8 time-of-flights experiments and average the resulting mobilities (see Figure SI10A). The simulated mobilities are then analysed with the GDM

$$\mu(T)|_{\sigma} = \mu_0 \exp\left(-\left(\frac{2}{3} \frac{\sigma_{\text{GDM}}}{k_B T}\right)^2\right) \quad (\text{SI 10.1})$$

which allows us to obtain  $\sigma_{\text{GDM}}$ . Strictly speaking, equation SI 10.1 is only true in the zero-field limit as  $\sigma_{\text{GDM}}$  is temperature-dependent<sup>4</sup>. Bässler demonstrated that relation SI 10.1 holds if the non-Arrhenius temperature-dependence  $\ln \mu \propto T^{-2}$  is still true<sup>4</sup> which is the case for the set of parameters in this study. Variations in the electronic coupling are neglected by this approach. It should be noted that the GDM analysis is used only to characterize the experimental disorder; another model could be used, but a new calibration of that model

would be needed to relate the apparent disorder of the system to an energetic disorder for transport simulations.

When plotting  $\sigma_{\text{GDM}}$  against  $\sigma$  we obtain an approximately linear relationship (see Figure SI10B). The energetic disorder  $\sigma_{\text{GDM}}$  of 77 meV (which we find experimentally for PCBM) can be translated into a  $\sigma$  of 135 meV.

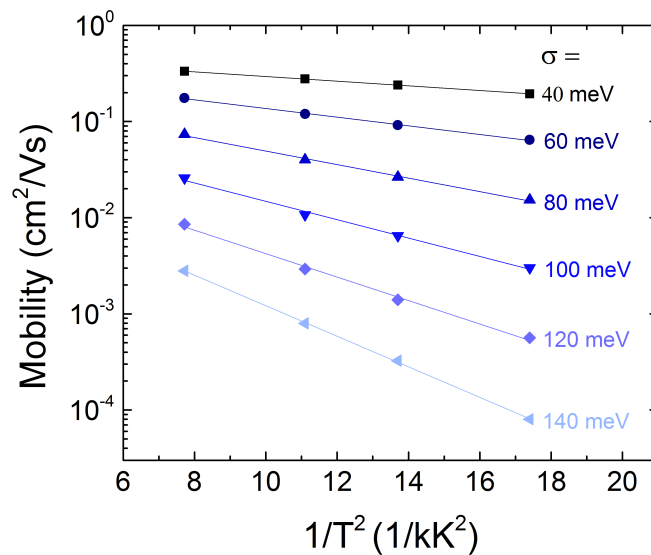


**Figure SI10A.** Mobility as a function of one over the squared temperature  $T$  for several energetic disorders  $\sigma$ . In the simulation  $\sigma$  defines the range of side energies  $E$  in the Marcus hopping rate.

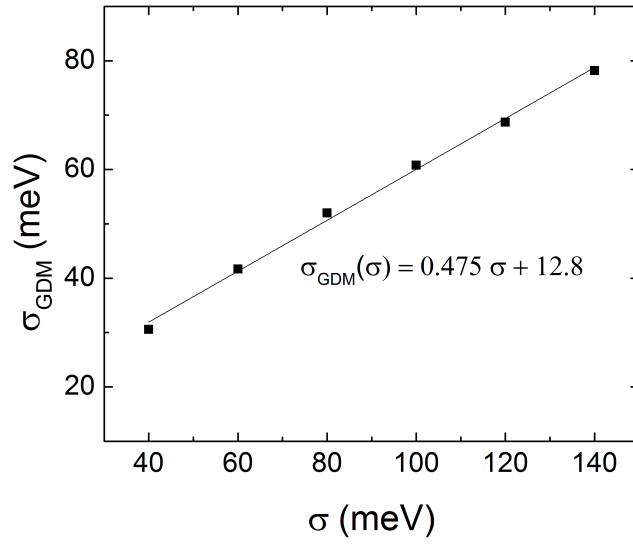


**Figure SI10B.** The mobility data of Figure SI10A is analysed with Gaussian Disorder Model (see formula SI 10.1) and an empirical energetic disorder  $\sigma_{\text{GDM}}$  is quantified. This leads to the depicted linear dependency between  $\sigma$  and  $\sigma_{\text{GDM}}$ .

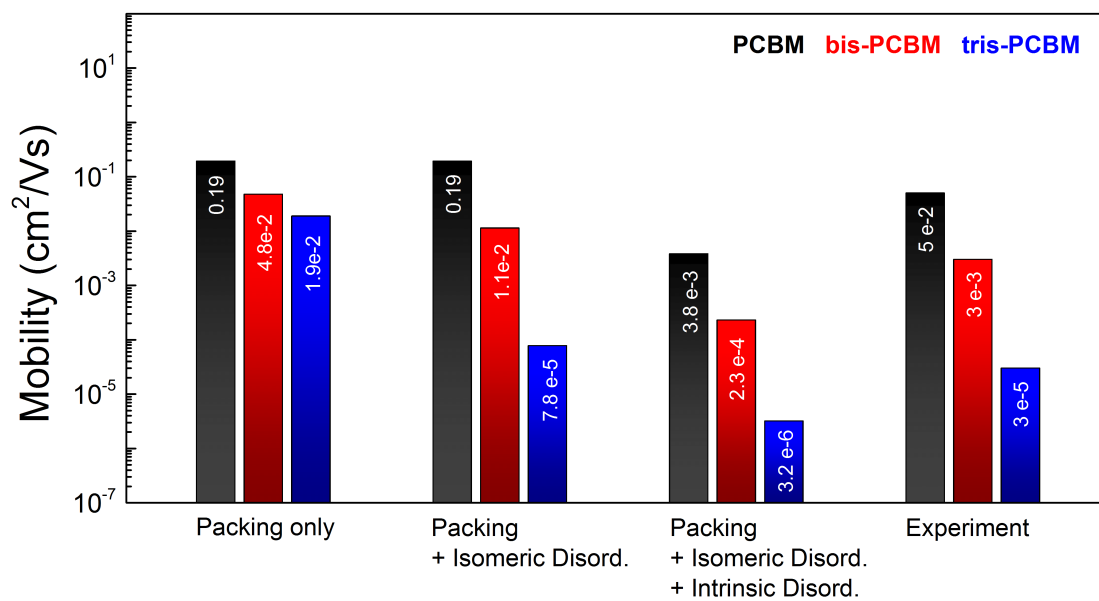
### SI11. Full table of charge-carrier mobilities for large MD structures

$\lambda = 200$ meV		M	B	T	B-E1	T-EEE
Packing disorder only	$\sigma$ (meV)	0	0	0	0	0
	$\mu$ (cm <sup>2</sup> /Vs)	4.75	1.22	4.87e-1	6.55e-1	2.61e-1
Isomeric disorder	$\sigma$ (meV)	0	56	121		
	$\mu$ (cm <sup>2</sup> /Vs)	4.75	2.78e-1	1.31e-3		
	$\sigma$ (meV)			72		
	$\mu$ (cm <sup>2</sup> /Vs)			4.00e-2		
Isomeric & implicit disorder	$\sigma$ (meV)	135	146	181		
	$\mu$ (cm <sup>2</sup> /Vs)	9.23e-3	5.67e-4	8.80e-6		

$\lambda = 500$ meV		M	B	T	B-E1	T-EEE
Packing disorder only	$\sigma$ (meV)	0	0	0	0	0
	$\mu$ (cm <sup>2</sup> /Vs)	1.93e-1	4.75e-2	1.88e-2	2.44e-2	1.02e-2
Isomeric disorder	$\sigma$ (meV)	0	56	121		
	$\mu$ (cm <sup>2</sup> /Vs)	1.93e-1	1.13e-2	7.75e-5		
	$\sigma$ (meV)			72		
	$\mu$ (cm <sup>2</sup> /Vs)			1.83e-3		
Isomeric & implicit disorder	$\sigma$ (meV)	104	118	160		
	$\mu$ (cm <sup>2</sup> /Vs)	3.79e-3	2.30e-4	3.34e-6		

**Table SI11.** Results for simulated mobility  $\mu$  for all cases studied on large molecular assemblies (100,000 molecules) and reorganisation energies  $\lambda$  of 200 meV and 500 meV. The value of  $\sigma$  represents the energetic disorder applied for each fullerene type and each level of disorder simulated (i.e., packing disorder only, isomeric disorder, isomeric and implicit disorder).



**Figure SI11.** Simulated charge transport data for reorganisation energies of  $\lambda = 500$  meV and structures containing 100,000 molecules. Bar chart compares the experimental results with the three different levels of disorder studied.

## SI12. Coarse grain fullerene force field

Here we extend the Girifalco<sup>10</sup> coarse grain buckminsterfullerene ( $C_{60}$ ) forcefield. The general principle in the creation of this simple forcefield is in the smearing out of the effective Lennards-Jones interactions of 60 graphitic-like carbons over the surface of a sphere the experimental size of a  $C_{60}$  fullerene. We believe this to be directly transferable to the interaction of the fullerene cages in functionalised adducts.

Our intent is to simulate the various PCBM adducts with a simple two-bead model for the fullerene cage and the side-chain, modelled entirely with Lennard-Jones interactions for computational efficiency. This model for the side-chain of a single spherical super-atom is likely to be better for more symmetric sidechains than PCBM such as indene-functionalised fullerenes.

We take the interaction parameters for the fullerene cage to be identical to those derived by Girifalco for  $C_{60}$ ; the atomistic model we use to inform about effective sidechain parameters that reproduce the exclusion of fullerene nearest neighbours seen in the radial distribution function.

We created an atomistic model for mono-PCBM based on the OPLS<sup>11</sup> empirical force- field, with the reference geometry from a gas-phase quantum chemistry calculation (b3lyp/6-31g\*), and the fullerene cage simulated as arbitrarily stiff. This we used to do molecular

dynamics on a small ensemble (2564 molecules, 20 ps of simulation time) to generate radial distribution functions which we used to fit the free parameters in our coarse-grain molecular dynamics model.

In our coarse-grain model, we choose the interaction energy of the sidechain bead to be the same as the Girifalco parameter for the fullerene site, scaled by the mass of the sidechain (190 Da versus 720.6 for C<sub>60</sub>).

We then compared coarse-grain radial distribution functions to the atomistic model, varying the effective bond length of the fullerene-sidechain connection, and the effective van-de-Waals radius of the sidechain.

$$V_{LJ} = 4\epsilon[(\sigma/r)^{12} - (\sigma/r)^6]$$

The complete set of parameters which describes the coarse grain forcefield is  $\epsilon_{C60} = 26.823$  kJ/mol,  $\sigma_{C60} = 0.895$  nm (Girifalco);  $\epsilon_{PBM} = 10.0$  kJ/mol,  $\sigma_{PBM} = 0.704$  nm; the C60-PBM bond being  $r = 0.64$  nm (fitted in this work).

Having fitted a coarse grain model for mono PCBM, we then extended this to the various fullerene isomer adducts by added extra mono-PCBM sidechain sites at the positions of the adducts.

The parameters for the irreducible set of bis and tris isomers were generated by computationally expedient direct enumeration of all possible configurations. Reduction of the set was made with a simple canonical representation.

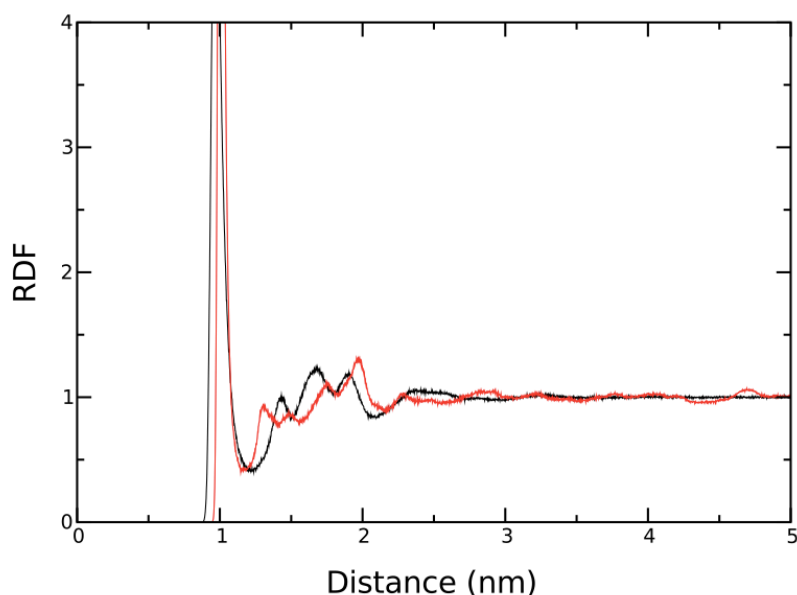


**Figure SI12A.** Radial distribution functions  $C_{60}$  centres for molecular dynamics simulations of both the coarse grain force field (black), and atomistic OPLS derived force field (red). Distributions for the atomistic representation were taken from the centre of mass of the 61 carbons making up the cage. The coarse grain representation is between the carbon pseudo atoms. The atomistic molecular dynamics was 2564 molecules over 20 ps of simulation time. The coarse grain simulation was 100'000 molecules over 200 ps of simulation time. We interpret the discrepancy between the nearest neighbour separation for the atomistic and coarse grain representations to be due to the approximate nature of our atomistic forcefield, which was not fitted to experimental fullerene separations but rather uses the default OPLS atom types with a stiff representation for the fullerene cage. Conversely, the coarse grain forcefield uses the carefully fitted Girifalco parameters.

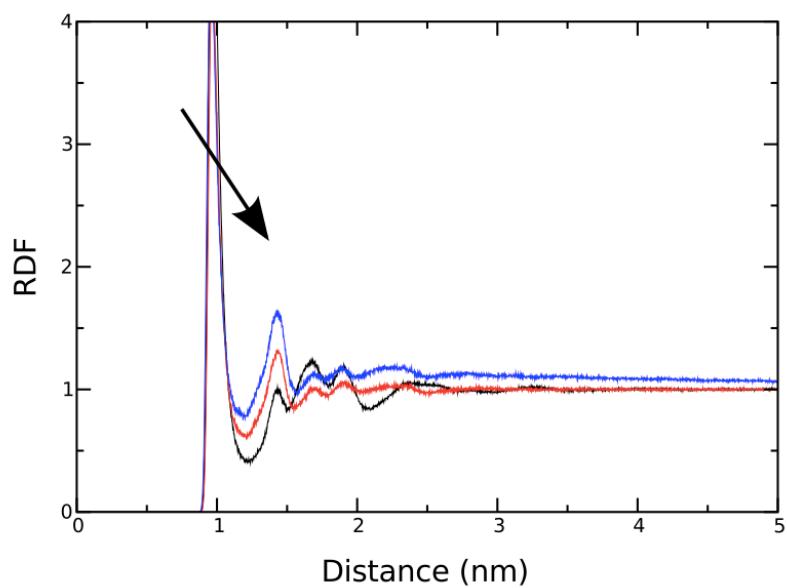


**Figure SI12B.** Radial distribution functions of  $C_{60} - C_{60}$  for mono (black), bis (red) and tris (blue). The effect of steric hindrance in the increasing number of sidechains can be seen in the decrease of nearest neighbours, and an increase in next nearest neighbours. The isomer pure mono phase has notably more structure than the mixed isomers of bis and tris.

### SI13. References for supporting information

- 1 K. Sakanoue, M. Motoda, M. Sugimoto, S. Sakaki, *J. Phys. Chem. A*, 1999, **103**, 5551.
- 2 J. Kirkpatrick, *Int. J. Quantum Chem.*, 2008, **108**, 51.
- 3 J. J. Kwiatkowski, J. Nelson, H. Li, J. L. Bredas, W. Wenzel, C. Lennartz, *Phys. Chem. Chem. Phys.*, 2008, **10**, 1852.
- 4 H. Bässler, *Phys. Stat. Sol. (B)*, 1993, **175**, 15.
- 5 T. D. Anthopoulos, D. M. de Leeuw, E. Cantatore, P. van 't Hof, J. Alma, J. C. Hummelen, *Journal of Applied Physics*, 2005, **98**.
- 6 J. M. Ball, R. K. M. Bouwer, F. B. Kooistra, J. M. Frost, Y. Qi, E. B. Domingo, J. Smith, D. M. de Leeuw, J. C. Hummelen, J. Nelson, A. Kahn, N. Stingelin, D. D. C. Bradley, T. D. Anthopoulos, *Journal of Applied Physics*, 2011, **110**.
- 7 S. M. Tuladhar, D. Poplavskyy, S. A. Choulis, J. R. Durrant, D. D. C. Bradley, J. Nelson, *Adv. Funct. Mater.*, 2005, **15**, 1171.
- 8 A. J. Campbell, D. D. C. Bradley, H. Antoniadis, *Appl. Phys. Lett.*, 2001, **79**, 2133.
- 9 V.D. Mihailetchi, J.K.J. van Duren, P.W.M. Blom, J.C. Hummelen, R.A.J. Janssen, J.M. Kroon, M.T. Rispens, E.J.H. Verhees, M.M. Wienk, *Adv. Funct. Mater.*, 2003, **13**, 43.
- 10 L. A. Girifalco, M. Hodak, R. S. Lee, *Phys. Rev. B*, 2000, **62**, 13104.
- 11 W. L. Jorgensen, D. S. Maxwell, J. Tirado-Rives, *J. Am. Chem. Soc.*, 1996, **118**, 11225.